A consistent pre-clinical/clinical elastography approach for assessing tumor mechanical properties in therapeutic systems

Jared A. Weis[a,b], Thomas E. Yankeelov[a-d], Samantha A. Munoz[c], Rahul A. Sastry[g], Stephanie L. Barnes[a,b], Lori R. Arlinghaus[a], Xia Li[a], and Michael I. Miga[a,c,f]

[a]Vanderbilt University Institute of Imaging Science, [b]Departments of Radiology and Radiological Sciences, [c]Biomedical Engineering, [d]Physics and Astronomy, [e]Cancer Biology, [f]Neurological Surgery, Vanderbilt University, Nashville, TN, USA

[g]Mechanical Engineering, Stanford University, Stanford, CA, USA

ABSTRACT

Unlike many other experimental imaging methods, elastography has enjoyed a strong link to the standard diagnostic and interventional evaluation technique of soft tissue palpation. As a result, the initial excitement about elastography quickly translated to clinical use (e.g., [1-3]) which now includes commercially available ultrasound and magnetic resonance (MR) elastography products. However, despite these advances, understanding what these macroscopic clinical-scale tissue measurements indicate with respect to the underlying cellular and tissue-matrix scale phenomena is largely unclear. In this work, we present preliminary data towards a more systematic study of the elasticity biomarker in characterizing cancer for therapeutic design and monitoring. In addition, we demonstrate that we can conduct these studies with techniques that are consistent across both pre-clinical (i.e., mouse) and clinical length scales. The elastography method we use is called modality independent elastography (MIE) [4, 5] and can be described as a highly translatable model-based inverse image-analysis method that reconstructs elasticity images using two acquired image volumes in a pre-post state of deformation. Quantitative phantom results using independent testing methods report an elastic property contrast between the inclusion and background as a 14.9 to 1 stiffness ratio with MIE reconstructing the ratio as 13.1 to 1. Preliminary elasticity reconstructions in murine and human systems are reported and are consistent with literature findings.

Keywords: breast cancer, mechanical properties, elastography, parameter reconstruction, mechanical model

1. INTRODUCTION

Elastography employs a combination of image and signal processing, and numerical methods to measure and analyze physical deformations in tissue such that a representation of the mechanical properties of the tissue of interest are generated [6-8]. In breast specifically, elastography has made real progress towards differentiation of benign and malignant breast lesions. For example, in studies involving hundreds of patients, elastography methods differentiated lesions with 100%, and 95% sensitivity and specificity, respectively, with excellent positive and negative predictive values [1] and with studies elsewhere having similar findings [9].

The underlying hypothesis of this work is that elastographic imaging can accurately and reliably monitor therapy-induced changes to breast cancer tissue architecture and as a result become an important therapeutic design tool and prognosticator. To support this goal, we believe an elastographic imaging methodology is needed to assist in pre-clinical and clinical evaluation such that it: (1) is robust and simple to implement, (2) can transcend murine-to-human length scales while retaining similar mechanical loading environments, and (3) is amenable to clinical workflow. Modality independent elastography (MIE), introduced by our group in [4, 5], is a highly translatable model-based inverse image-analysis method that reconstructs elasticity images of tissue by incorporating a biomechanical finite element model into the non-rigid registration of two image volumes acquired under different static loading environments. We suggest that MIE is an excellent candidate to fill this role. In order to perform the model-based inverse image-analysis MIE reconstructions, there is a critical need to impart deformations on the tissue system that can be replicated within the computational system. This has been a considerable barrier towards reliable MIE reconstruction. With our recent finding that non-rigid image registration methods can be used to automatically resolve boundary conditions for MIE [10], there

is a clear pathway for an easy-to-apply, but perhaps geometrically complex, deformation source. This work presents the first experimental application of this novel MIE framework in phantom, murine, and clinical data.

2. METHODS

2.1 MIE approach

The MIE method is an image analysis technique that analyzes two anatomical image volumes whereby the only difference is the application of a mechanical compression. Biomechanical computer models under a Hookean linear elastic assumption are used to iteratively deform the pre-compression image volume until it matches the acquired post-compression image volume using an image volume zone-based image similarity metric. Once reconstruction is complete, the output is a distribution of mechanical properties. As we are using MIE in a complementary role to conventional imaging, *a priori* information (spatial priors) from the MR signal intensity data are used to group regions for property reconstruction. A demons non-rigid registration framework [11] is used to register the post-compression image volume to the pre-compression image volume and the boundary conditions used to drive the biomechanical finite element model during MIE reconstruction are automatically extracted from the non-rigid deformation field. For more extensive discussion regarding the MIE computational methodology, the interested reader is referred to previous work by our group [4, 5, 10, 12-15].

2.2 Gel phantom data

MIE gel phantoms were created by submerging a stiff 2% w/v agarose gel inclusion within a softer 1.5% w/v agarose gel background. Phantoms were created with a diameter of approximately 22mm and height of approximately 13mm. MRI was performed using a Varian 7.0T scanner (Varian, Palo Alto, CA) with a 38-mm quadrature coil. Images were acquired before and after compression using a fast spin echo sequence. Compression was applied through the use of a custom-built gel deformation chamber. Separate samples of both the inclusion and background gel material were subjected to material testing using an Enduratec Electroforce 3100 mechanical tester (Bose, Enduratec Systems Group, Minnetonka, MN).

2.3 Murine data

A murine tumor model of triple-negative breast cancer was used whereby 4 to 6 week old female athymic nude mice (Harlan, Indianapolis, IN) were injected subcutaneously in the right flank with approximately 10^7 MDA-MB-231 cells in a 30% Matrigel suspension. Tumors were allowed to grow for 8-10 weeks. MRI was performed using a Varian 7.0T scanner (Varian, Palo Alto, CA) with a 38-mm quadrature coil. Anatomical images were acquired before and after compression using a fast spin echo sequence. Compression was applied by a 5cc balloon catheter controlled by a syringe driver that was placed within the MR imaging coil in close proximity to the tumor. All animal procedures were approved by the Institutional Animal Care and Use Committee.

2.4 Clinical data

Patients with no previous systemic therapies for breast cancer and histologically documented invasive carcinoma of the breast were eligible for the study. MRI was performed using a Philips 3T Achieva MR scanner Philips Healthcare, Best, The Netherlands). T_1 weighted structural data was acquired before and after compression *via* a 192×192×160 acquisition matrix with isotropic voxel size of 1.0 mm^3. Compression was applied through the use of a custom-built bladder that imparts gentle deformations to the breast within the MR imaging coil [14]. Participating patients provided informed written consent to an Institutional Review Board approved study.

3. RESULTS

While conceptually clear, MIE has had challenging barriers. Previously, we developed mechanical devices for controlled deformation delivery to soft-tissue such that boundary conditions to the computer model would be simple. While successful in some instances, it proved to be difficult and not easy to translate. In a fundamental innovation using non-rigid image registration methods to overcome this barrier concerning boundary condition deployment, we see the result in Figure 1. Figure 1 illustrates the MIE method as applied to an agarose gel phantom containing a stiff inclusion within

a softer background gel. In Figure 1, we see 3D volume renderings of the cylindrical phantom before (Figure 1A) and after (Figure 1C) deformation. Figure 1B and Figure 1D reflect central-slice 2D data showing the agarose inclusion. Note the complicated geometry of deformation applied to the phantom as indicated by the white arrowhead in Figure 1C. In Figure 1E, the MIE elasticity reconstruction can be seen clearly showing the stiffer inclusion. The elastic property contrast between inclusion and background measured using independent mechanical testing was a 14.9 to 1 elastic stiffness ratio. The results from MIE reconstruction estimated the ratio as 13.1 to 1, which results in very good agreement.

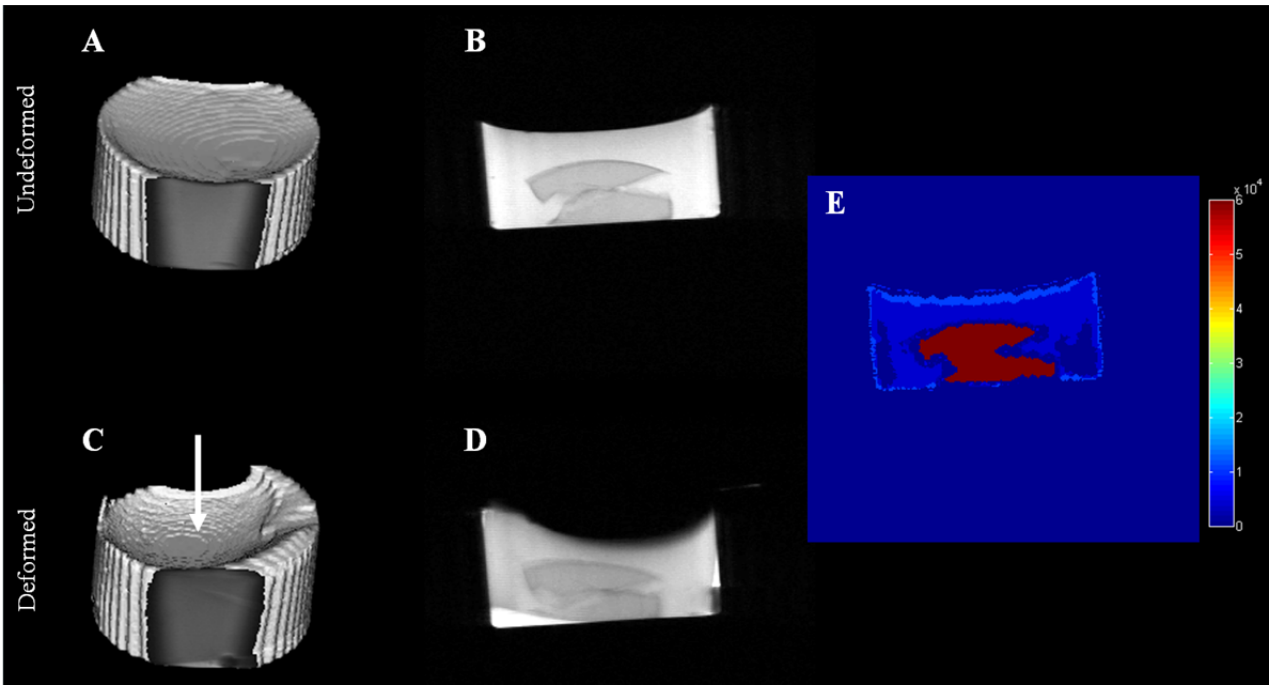

Figure 1. Pre/post deformation data and respective MIE reconstructions for phantom data. 3-D volume and central 2-D slice of undeformed (A and B, respectively) and deformed (C and D, respectively) MR datasets. The area of deformation application is highlighted by the white arrowhead. MIE reconstruction (E) was performed using *a priori* intensity-based regions. The colorbar ranges from 0-60 kPa.

Convergence plots, shown in Figure 2, detail the operational nature of the MIE methodology for the gel phantom data. Spatial prior intensity data, through six regions of iso-intensity in the undeformed MR image (Figure 2A), are segmented into regions (Figure 2B) defining the resolution of the reconstruction. Elastic properties for each region are reconstructed (Figure 2C) and overall similarity metric convergence history (Figure 2D) and individual property convergence history (Figure 2E) are shown. The elastic property iteration history shows initialization of the reconstruction at a uniform initial guess followed by *a priori* domains reacting dynamically to maximize image similarity. It is interesting to note that while the reconstruction reflects six degrees of freedom for the two property gel phantom, the reconstruction is correctly convergent towards two independent properties.

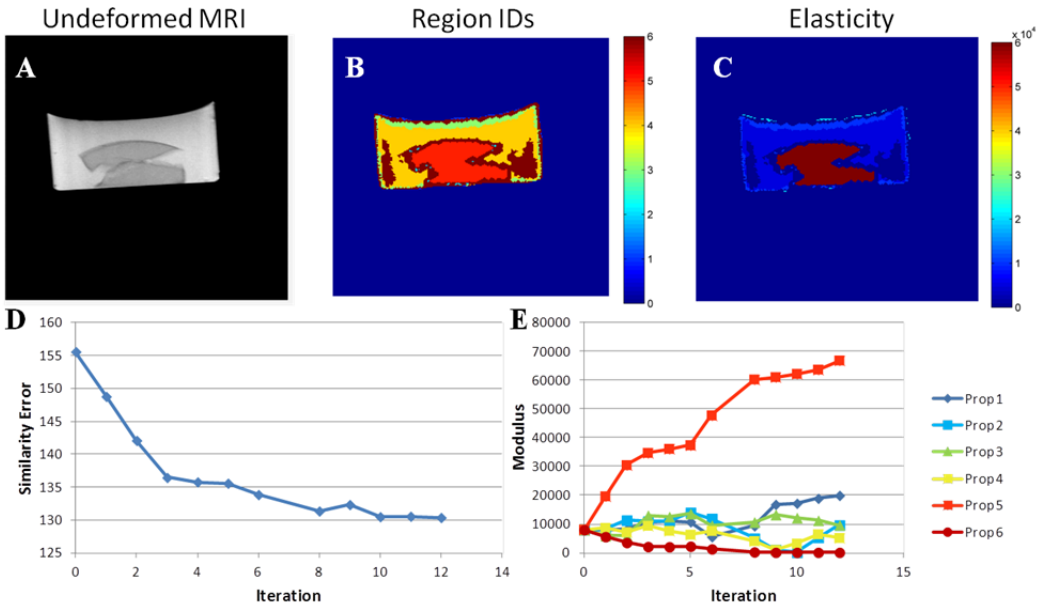

Figure 2. MIE reconstruction operational convergence history for gel phantom data. The undeformed MR image (A) is segmented into six spatial prior iso-intensity regions (B) and a MIE reconstruction is performed (C). Similarity metric error (D) over the iterative history of the reconstruction shows convergence. Region property reconstruction history (E) shows initialization at uniform initial guess, followed by convergence towards two independent properties.

Figure 3 illustrates the application of MIE on a murine hind-flank triple negative breast cancer xenograft tumor model. Figure 3 shows 3D volume renderings of the cylindrical phantom before (Figure 3A) and after (Figure 3C) deformation. Figure 3B and Figure 3D reflects central-slice 2D data showing the agarose inclusion. We again direct the reader to the complicated geometry of deformation applied to the tumor as indicated by the white arrowhead in Figure 3C. In Figure 3E, the MIE elasticity reconstruction can be seen for the murine tumor. In this murine hind-flank tumor model, we see expected low stiffness values produced in the central necrotic region (as confirmed by histology) with elevated values in the tumor parenchyma.

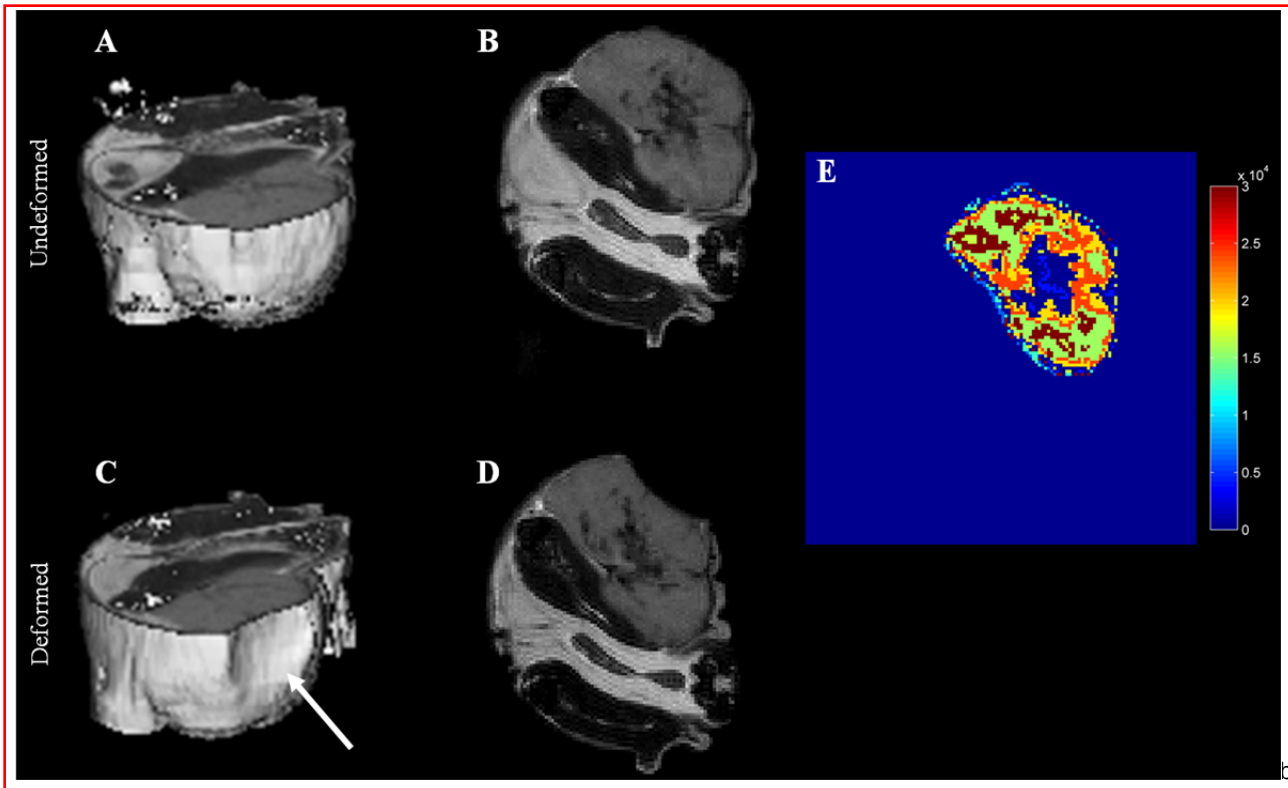

Figure 3. Pre/post deformation data and respective MIE reconstruction for murine tumor data with experimental mouse system. 3-D volume and central 2-D slice of undeformed (A and B, respectively) and deformed (C and D, respectively) MR datasets. The area of deformation application is highlighted by the white arrowhead. MIE reconstruction (E) was performed using *a priori* intensity-based regions. The colorbar ranges from 0-30 kPa.

As indicated above, the challenge of a validated approach applied consistently over the murine and clinical length scale is difficult. Here, we also demonstrate that our automated MIE approach is adaptable to the clinic. Figure 4A-C show a clinical prototype deformation source. Figure 4D,E is a volume rendering of the breast with sagittal cross-section of the tumor before the application of deformation, respectively. Figure 4F,G is the deformed counterparts. The area of geometrically complex deformation application can be seen designated by the black arrowhead in Figure 4F. The MIE reconstruction can be seen in Figure 4H. A section of the patient's breast tumor can be clearly seen in both the central-slice structural MR data of Figure 4E and the corresponding MIE reconstruction in Figure 4H and is observed to exhibit greatly enhanced stiffness over the surrounding adipose and fibroglandular tissue.

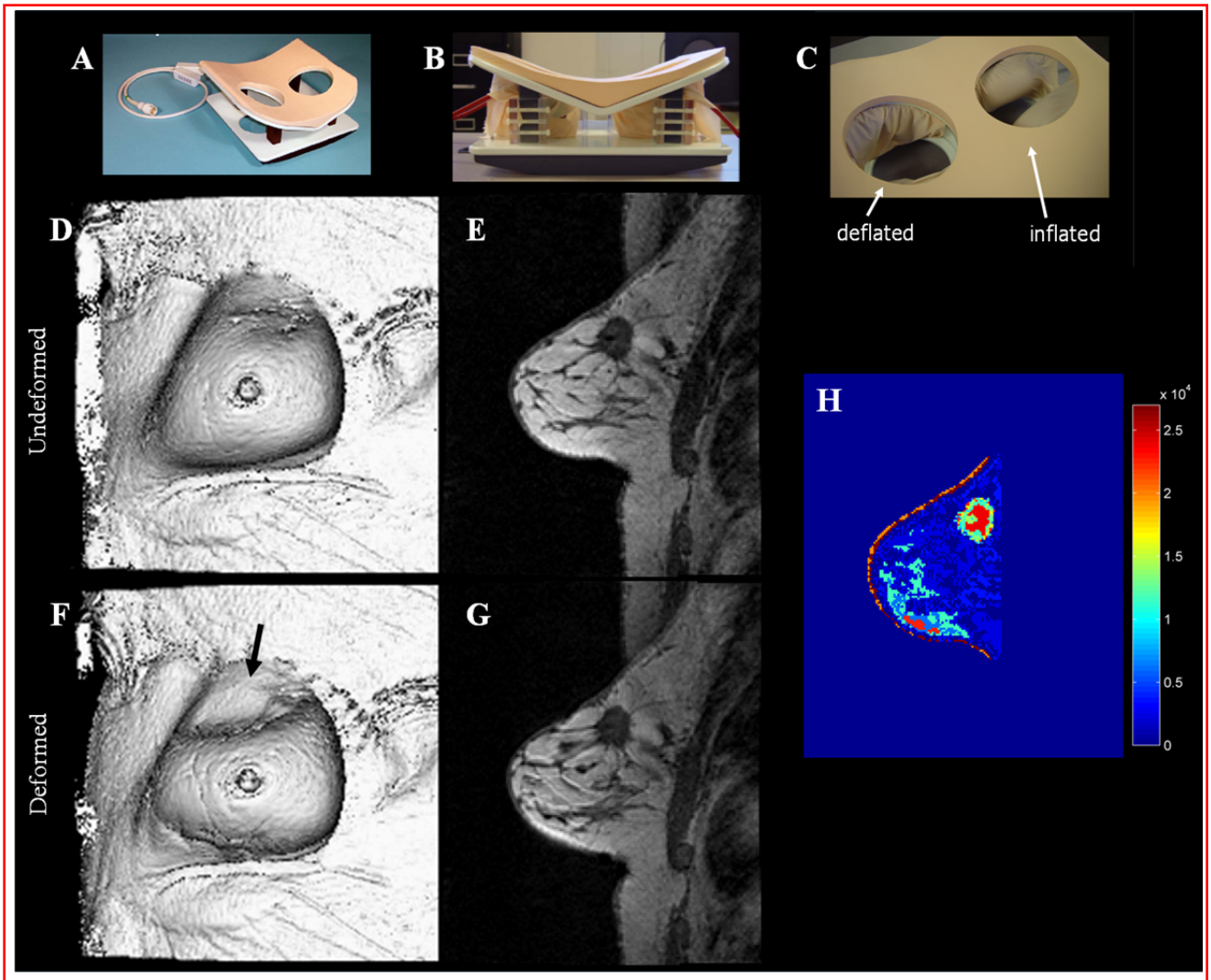

Figure 4. Prototype clinical deformation device (A-C) and pre/post deformation data with respective MIE reconstruction for human breast tumor. 3-D volume and central 2-D slice of undeformed (D and E, respectively) and deformed (F and F, respectively) MR datasets. The area of deformation application is highlighted by the black arrowhead. MIE reconstruction (H) was performed using *a priori* intensity-based regions. The colorbar ranges from 0-27 kPa.

4. CONCLUSIONS

While MIE was introduced our group in [4, 5] and has been under investigation for several years [12-15], recent breakthroughs towards automation [10] have fundamentally improved its ability to be translated and applied consistently across differing length scales. These results represent the first experimental application of the novel automated MIE reconstruction framework, with exciting preliminary data in phantom, murine, and human applications shown here. This analysis was not possible in the past due to the boundary condition mapping problem. Several approaches were tried in the past [16, 17] but only until [10] were such encouraging results possible.

The *in vivo* pre-clinical and clinical results are very consistent with observational work in the literature. We also show agreement with the quantitative comparison in phantom data as compared to independent mechanical testing. Based on the level of automation and translation, we believe MIE provides consistent mechanical property measurements across pre-clinical (i.e. murine) and clinical length scales and is capable of integration with other complimentary modalities, which could be invaluable towards design, monitoring, and prediction of outcomes for therapeutic agents.

ACKNOWLEDGEMENTS

We offer our sincerest appreciation to the patients who selflessly volunteered to participate in this study. This work was supported by the National Institutes of Health, the National Cancer Institute by R01CA138599, R25CA092043, U01CA142565, and the Vanderbilt initiative in Surgery and Engineering Pilot Award Program. We thank the Kleberg Foundation for generous support of the imaging program at our Institution.

REFERENCES

[1] R. G. Barr, "Real-time ultrasound elasticity of the breast: initial clinical results," *Ultrasound Q*, vol. 26, pp. 61-6, Jun 2010.
[2] R. G. Barr, S. Destounis, L. B. Lackey, 2nd, W. E. Svensson, C. Balleyguier, and C. Smith, "Evaluation of breast lesions using sonographic elasticity imaging: a multicenter trial," *J Ultrasound Med*, vol. 31, pp. 281-7, Feb 2012.
[3] M. Yin, J. A. Talwalkar, K. J. Glaser, A. Manduca, R. C. Grimm, P. J. Rossman, J. L. Fidler, and R. L. Ehman, "Assessment of hepatic fibrosis with magnetic resonance elastography," *Clinical Gastroenterology and Hepatology*, vol. 5, pp. 1207-1213, 2007.
[4] M. I. Miga, "A new approach to elastographic imaging: Modality independent elastography," *Medical Imaging 2002: Image Processing: Proc. of the SPIE*, vol. 4684, pp. 604-611, 2002.
[5] M. I. Miga, "A new approach to elastography using mutual information and finite elements," *Phys Med Biol*, vol. 48, pp. 467-80, Feb 21 2003.
[6] M. Bilgen, "Target detectability in acoustic elastography," *IEEE Trans Ultrason Ferroelectr Freq Control*, vol. 46, pp. 1128-33, 1999.
[7] M. M. Doyley, P. M. Meaney, and J. C. Bamber, "Evaluation of an iterative reconstruction method for quantitative elastography," *Phys Med Biol*, vol. 45, pp. 1521-40, Jun 2000.
[8] E. E. Konofagou and J. Ophir, "Precision estimation and imaging of normal and shear components of the 3D strain tensor in elastography," *Phys Med Biol*, vol. 45, pp. 1553-63, Jun 2000.
[9] A. Itoh, E. Ueno, E. Tohno, H. Kamma, H. Takahashi, T. Shiina, M. Yamakawa, and T. Matsumura, "Breast disease: clinical application of US elastography for diagnosis," *Radiology*, vol. 239, pp. 341-50, May 2006.
[10] T. S. Pheiffer, J. J. Ou, R. E. Ong, and M. I. Miga, "Automatic Generation of Boundary Conditions Using Demons Nonrigid Image Registration for Use in 3-D Modality-Independent Elastography," *Ieee Transactions on Biomedical Engineering*, vol. 58, pp. 2607-2616, Sep 2011.
[11] J. P. Thirion, "Image matching as a diffusion process: an analogy with Maxwell's demons," *Med Image Anal*, vol. 2, pp. 243-60, Sep 1998.
[12] C. W. Washington and M. I. Miga, "Modality independent elastography (MIE): A new approach to elasticity imaging," *Ieee Transactions on Medical Imaging*, vol. 23, pp. 1117-1128, Sep 2004.
[13] M. I. Miga, M. P. Rothney, and J. J. Ou, "Modality independent elastography (MIE): Potential applications in dermoscopy," *Medical Physics*, vol. 32, pp. 1308-1320, May 2005.
[14] J. J. Ou, "Development of Modality-Independent Elastography as a Method of Breast Cancer Detection," in *Biomedical Engineering*. vol. Ph.D. Nashville: Vanderbilt University, 2007, p. 179.
[15] J. J. Ou, R. E. Ong, T. E. Yankeelov, and M. I. Miga, "Evaluation of 3D modality-independent elastography for breast imaging: a simulation study," *Physics in Medicine and Biology*, vol. 53, pp. 147-163, Jan 7 2008.
[16] R. E. Ong, J. J. Ou, and M. I. Miga, "Using Laplace's equation for non-rigid registration of breast surface," *Medical Imaging 2007: Visualization and Image-guided Procedures: Proc. of SPIE*, vol. 6509, 2007.
[17] R. E. Ong, J. J. Ou, and M. I. Miga, "Non-rigid registration of breast surfaces using the laplace and diffusion equations," *Biomedical Engineering Online*, vol. 9, Feb 12 2010.